Transactions, **SMiRT-26**
Berlin/Potsdam, Germany, July 10-15, 2022
Division V

COMPARISON OF IN-STRUCTURE RESPONSE SPECTRA BASED ON NUMERICAL MODELS AND RECORDED DATA WITH EMPIRICAL METHODS

Asa Bassam[1], Siavash Dorvash[2], Benjamin D. Kosbab[3]

[1] Senior Project Manager, Simpson Gumpertz & Heger, Atlanta, GA, USA (abassam@sgh.com)
[2] Senior Consulting Engineer, Simpson Gumpertz & Heger, Newport Beach, CA, USA
[3] Principal, Simpson Gumpertz & Heger, Atlanta, GA, USA

ABSTRACT

This paper compares horizontal in-structure response spectra (ISRS) obtained from probabilistic transient analyses of the numerical model of an example nuclear plant low-rise shear-wall structure and the ISRS obtained from the recorded accelerations in an instrumented low-rise shear-wall building with those from standards-based simplified empirical methods outlined in IAEA-TECDOC-348 (1985) and ASCE 7 (2022). The goal is to explore whether alternative, simplified procedures for ISRS generation other than numerical models and transient analysis might be suitable for broader use in the nuclear industry.

INTRODUCTION

Traditional methods for obtaining ISRS in nuclear plant structures, developed over the last five decades, rely on transient analyses of detailed numerical structural models and computing acceleration response time histories at various locations of interest. The expected detail and complexity of these numerical models and corresponding analysis and post-processing steps have increased as recognition of underlying uncertainties and characteristics of building response has evolved. These uncertainties include but are not limited to the flexibility of floor slabs, mass and stiffness irregularities, uncaptured components of the ground motion, intensity and frequency content of the ground motions, level of inelastic behavior, distribution of seismic damage, the contribution of non-structural components such as partition walls to the building stiffness, soil-structure interaction effects, damping mechanisms, and potential interactions of the non-structural components and equipment. These parameters can potentially alter the amplitude and frequency content of the floor motions, affecting the ISRS. Although current practices are expected to produce conservative and safe designs, it is not clear whether the rigor in transient analysis results in physically accurate estimates of ISRS or not.

In parallel to the development of traditional ISRS generation methods relying on transient analysis, an increasing number of seismically instrumented buildings have been subjected to actual earthquakes and have collected physical response data. For example, the Center for Engineering Strong Motion Data (CESMD) (2022) provides a relatively large set of recorded data for various buildings. These broad sets of data, combined with analytical solutions of simplified system models, have permitted the development and refinement of alternative methods for approximating structure ISRS. Such alternative methods are used for seismic design and qualification of non-structural elements in non-nuclear industries (e.g., via ASCE 7 (2022) and its underlying basis document NIST GCR 18-917-43 (2018) and limited application in non-power nuclear facilities (e.g., via IAEA-TECDOC-348 (1985)). These methods are efficient and straightforward and do not require detailed numerical models or transient analysis. They work best when a building is dominated by one mode in each horizontal direction. Given the inherent uncertainties in predicting in-structure demands on components housed inside a building subjected to a seismic event, one may ask whether a difference in accuracy warrants the use of complex numerical models and transient analysis compared with the simplicity of alternative empirical methods.

This paper aims to demonstrate how reasonably one can estimate the ISRS from the empirical methods instead of an extensive SSI model that includes all details and uncertainties in the soil and structural properties. The advantage of using the empirical methods is the significant savings in the computational resources, project time, and cost by avoiding the generation of detailed numerical models needed to generate the response. Since the empirical methods and the instrumentation data are primarily available for the horizontal response only at this time, this study considers horizontal response only, and the evaluation of the vertical response is not part of the current study.

EMPIRICAL APPROACHES FOR OBTAINING ISRS

ASCE 7 (2022) Procedure

A simplified procedure is provided in Chapter 13 of ASCE 7 (2022) to estimate the maximum acceleration to be used to design non-structural components attached at a given height of the building. The non-structural components are self-supporting structures other than the building. Equation 13.3-1 of ASCE 7 (2022) provides an empirical formula to estimate the horizontal seismic design force as:

$$F_P = 0.4 S_{DS} I_P W_P \left[\frac{H_f}{R_\mu}\right] \left[\frac{C_{AR}}{R_{PO}}\right] \tag{1}$$

where F_P = Seismic design force; S_{DS} = Short period spectral acceleration as determined per Section 11.4.5 ASCE 7-22; I_P = Component Importance Factor as determined per Section 13.1.3 of ASCE 7-22; W_P = Component operating weight; H_f = Factor for force amplification as a function of height in the structure as determined in Section 13.3.1.1 of ASCE 7-22; R_μ = Structure ductility reduction factor as determined in Section 13.3.1.2 of ASCE 7-22; C_{AR} = Component resonance ductility factor that converts the peak floor or ground acceleration into the peak component acceleration, as determined in Section 13.3.1.3 of ASCE 7-22; and R_{PO} = Component strength factor as determined in Section 13.3.1.4 of ASCE 7-22.

Based on Equation (1), the equivalent peak spectral acceleration of the ISRS can be estimated as the ratio of F_P/W_P with R_{PO} =1, and replacing S_{DS} with the peak foundation input response spectrum, S_{FIRS}:

$$S_a = 0.4 S_{FIRS} I_P \left[\frac{H_f}{R_\mu}\right] . C_{AR} \tag{3}$$

IAEA-TECDOC-348 (1985) Procedure

Another simplified procedure is provided in Chapter 8 of IAEA-TECDOC-348 to estimate the ISRS to be used to design a piece of equipment attached to the building at a given height. Using this procedure, the spectral acceleration of the ISRS can be obtained as:

$$S_a = C_{Di} D_4 = (D_1 D_2 D_3 D_4)/\mu_d \tag{4}$$

where D_1 is the Response Factor which is the ratio of the peak to PGA of the input spectrum; D_2 is a coefficient related to the building damping; $D_3 = 1 + 0.5(\frac{equipmentheight}{building\ height})$; D_4 is an amplification factor due to floor response spectrum as shown in Figure 1; and μ_d is the expected building ductility. The parameter A_f in Figure 1 is a function of the building and equipment damping ratios, their effective mass ratio, and their ductility.

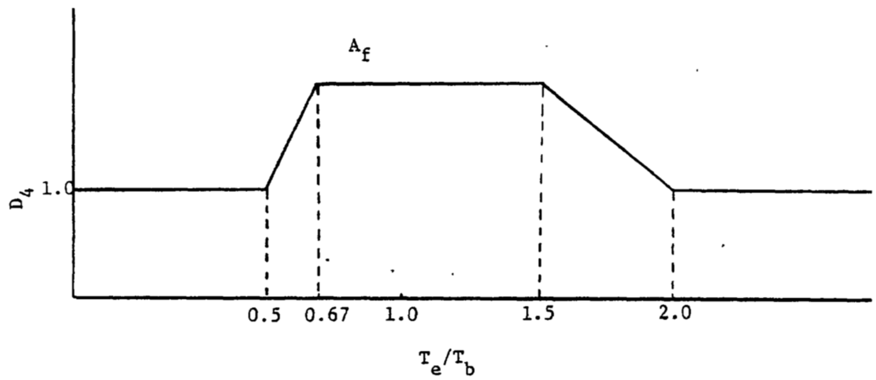

Figure 1. Parameter D_4 in IAEA-TECDOC-348 (1985)

CASE STUDIES

A common type of structure in many nuclear power plants is the low-rise concrete shear wall building. Therefore, the case studies in this paper focus on this type of structure to evaluate the validity of the empirical procedures for estimating the ISRS for nuclear structures. In these case studies, the ISRS obtained from numerical analyses (Case Study 1), and the recorded acceleration data from instruments during actual earthquakes (Case Study 2), are compared with those obtained from the empirical methods by IAEA-TECDOC-348 (1985) and ASCE 7 (2022).

Table 1 shows the parameters used to calculate the peak spectral acceleration of the ISRS at the roof of the buildings in the case studies, using the ASCE 7 (2022) approach. Similarly, Table 2 shows the parameters used to calculate the ISRS at the roof of the buildings in the case studies using the IAEA TECDOC-348 (1985) approach.

Table 1: Input Parameters Used for the ASCE 7 (2022) Method of the Floor Spectral Acceleration

Input Parameters	Value	Applicable Section of ASCE 7 (2022)
I_P	1.5	Section 13.1.3
C_{AR}	2.2	Table 13.6.1
H_f	3.5	Equation 13.3-4
R_μ	1.3	Equation 13.3-6

Table 2: Input Parameters Used for the IAEA-TECDOC-348 (1985) Method of the ISRS Calculation

Input Parameters		Value	Applicable Section of IAEA-TECDOC-348 (1985)
Equipment ductility	μ_e	2	Equation 8.2
Building ductility	μ_b	2.2	Table 7.3
D_2		1	Table 7.5
D_3		1.5	Equation 7.5

CASE STUDY 1

The first case study compares the ISRS obtained from a detailed three-dimensional (3D) probabilistic Soil-Structure Interaction (SSI) analysis of a Diesel Generator Building (DGB) of a nuclear power plant with those obtained from the empirical methods by IAEA-TECDOC-348 (1985) and ASCE 7 (2022).

Description of the model and input data

The building used in this case study is a rectangular 34.5 ft. tall, two-story reinforced concrete shear wall structure with plan dimensions of about 135 ft. by 90 ft. It is modeled as a surface-founded structure. Figure 2 presents a 3D isometric view of the FE model and the cross-sectional elevation view of the DGB. A summary of the median structural material properties and the coefficient of variation is provided in Table 3.

The top 10 ft. of soil profile under the building foundation consists of relatively soft soil with a shear-wave velocity of approximately 300 ft/s, followed by 10 ft. of slightly stiffer soil with an average shear-wave velocity of about 650 ft/s, and 10 ft. of relatively stiff soil with an average shear-wave velocity of about 2000 ft/s. The average V_{S30} for the soil material is about 385 ft/s with a logarithmic standard deviation range between 0.30~0.80 (varying between individual soil layers). The detailed description of the soil properties is outside of the scope of this paper.

The uncertainties in the SSI input parameters are captured by sampling these SSI input parameters on their respective distributions to generate model and soil variations, and each variation (case) is uniquely paired to an input time history. 30 SSI cases are developed by Latin Hypercube Sampling (LHS) of the randomized soil and structural input parameters. Based on LHS, each soil or structural parameter is sampled on its respective distribution and divided into 30 equal probability bins from -2σ to +2σ. Thirty sets of ground motions consistent with the foundation input spectra (Figure 3) are also developed for probabilistic SSI analyses. These 30 sets of ground motions are randomly and uniquely paired to the 30 randomized SSI models.

Case study 1 results

For each SSI analysis case, the co-directional ISRS due to input motions in three orthogonal directions were computed at each selected node through algebraic summation of the time histories in each direction resulting from input motions in all three directions. This was accomplished by extracting the acceleration time histories in all three directions due to the input motion in each direction (9 total) and adding the accelerations algebraically in each direction at each time step. The ISRS were then calculated based on the co-directional time histories that were generated in each direction.

The SSI analyses indicated the dominant frequencies of the SSI system of about 3 Hz. This frequency is mainly dominated by the frequency response of the soil and is, therefore, approximately the same in both N-S and E-W directions.

Figure 4 shows the average ISRS response at 5% damping at the roof of the building model. It also shows the empirical ISRS results obtained from the procedures in IAEA TECDOC 1348 and ASCE 7-22. The same figure also shows the building input spectra at the foundation elevation.

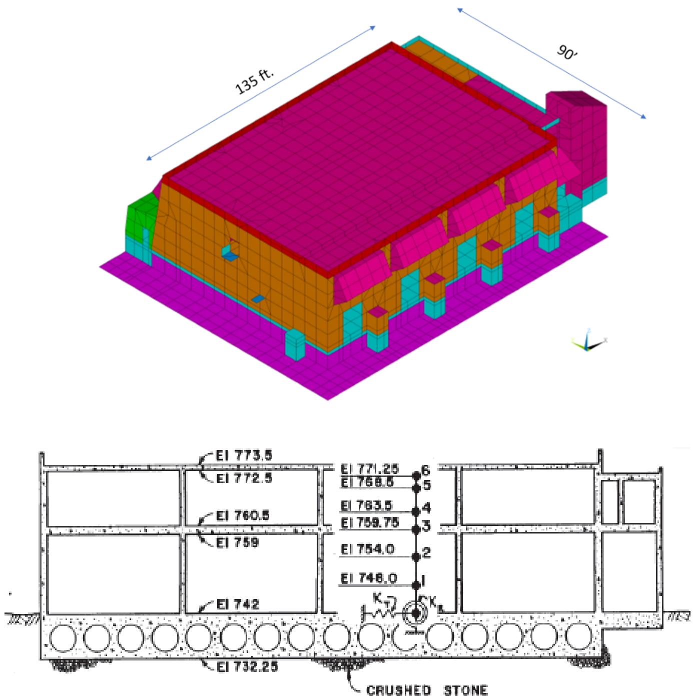

Figure 2. FE Model Isometric View (Top) and Elevation Section View (Bottom) of the Building Used for Numerical ISRS Computation

Table 3: Structural Material Properties Used in the Numerical Model

Material	Elastic Modulus (ksf)	Poisson's Ratio	Damping Ratio	Logarithmic Standard Deviation	
				Elastic Modulus	Damping
Concrete	500,000	0.25	0.07	0.4	0.35

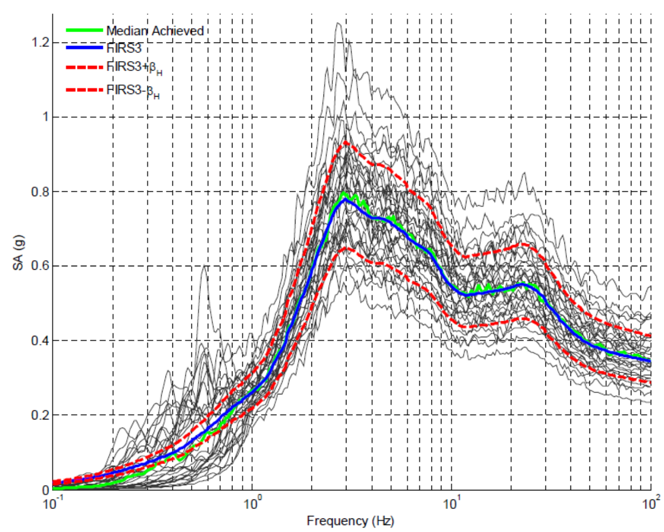

Figure 3. Response Spectra of the Input Motions Used in the Numerical Analyses

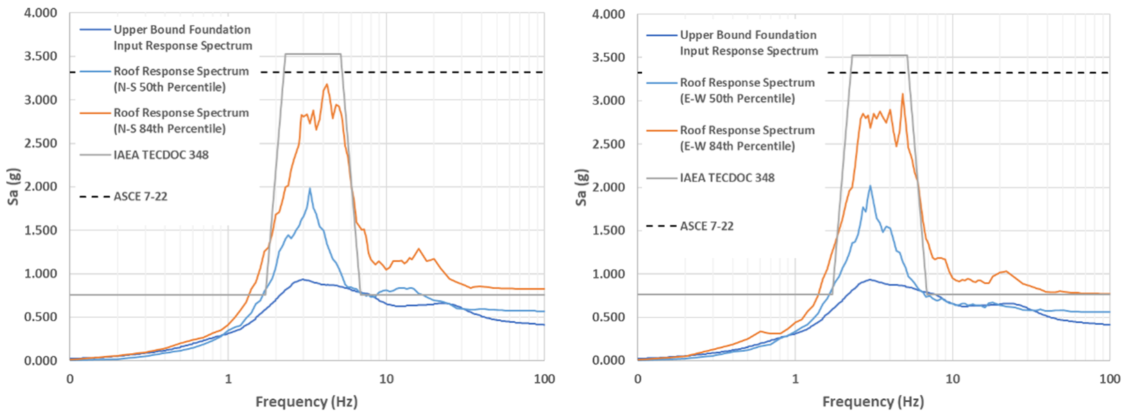

Figure 4. Comparison of the 5% Damping ISRS Computed from the Numerical Analyses with the Empirical Methods and the Foundation Input Spectra, N-S Direction (Left) and E-W Direction (Right)

As can be seen, both ASCE 7 (2022) and IAEA-TECDOC-348 (1985) methods result in similar peak spectral accelerations. The results of these empirical methods also agree reasonably well with the 84th percentile peak spectral acceleration obtained from probabilistic numerical analyses, although they are somewhat more conservative. The PGA of the ISRS from IAEA-TECDOC-348 PGA is also fairly close to the 84th percentile PGA obtained from the probabilistic numerical analyses.

CASE STUDY 2

The second case study compares the recorded ISRS obtained from an instrumented low-rise concrete building with those obtained from the empirical methods by IAEA-TECDOC-348 (1985) and ASCE 7 (2022).

Description of the structure and input data

The building used in this case study is a rectangular 48 ft. tall, three-story reinforced concrete shear wall structure with plan dimensions of about 162 ft. by 79 ft. The floor system consists of 3-inch reinforced concrete slabs at each story and a 2.75-inch reinforced concrete slab at the roof. The building is a surface-founded structure, and the foundation type is spread footing. Figure 2 shows a photo of the building and the schematic plan and elevation views. The small arrows indicate the locations and directions of the accelerometers installed throughout this building.

Case study 2 results

There are five earthquake records available for this building in the CESMD (2022) database. These earthquakes and their dates of occurrence and magnitudes are shown in Table 4. The response spectra of the recorded accelerations at the foundation of the instrumented building from the five available earthquake records in the CESMD (2022) database are shown in Figure 6. Similarly, the ISRS of the recorded accelerations at the roof of the instrumented building from the five earthquake records in CESMD (2022) are shown in Figure 7. These spectra are scaled (anchored) to 0.5g peak ground acceleration (PGA) which is the site-specific design PGA at the location of the instrumented building (Taft, CA) from the USGS hazard maps (obtained from the ASCE 7 hazard tool (2022).

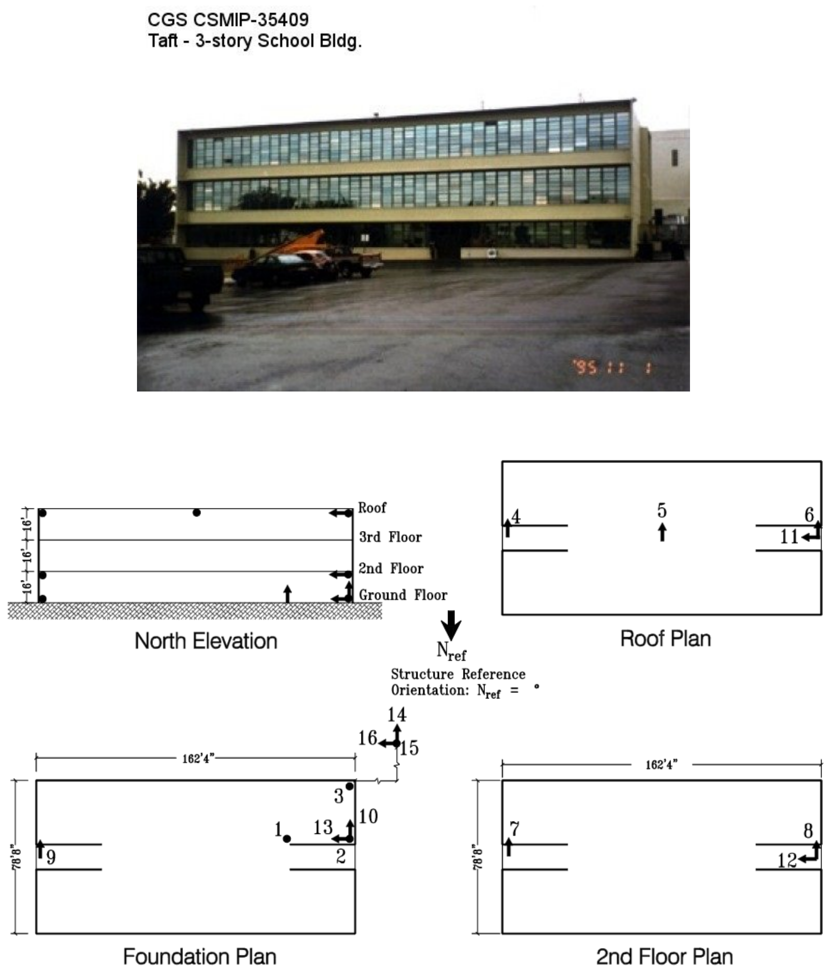

Figure 5. Photo of the Instrumented Building (Top) and Schematic Elevation and Plan Views (Bottom)

The ISRS results show very distinct peaks at the frequency of 5 Hz, and 4.2 Hz in the N-S and E-W directions, respectively, indicating that these are the dominant frequencies of the instrumented building in these directions.

Figure 8 compares the average (mean) and envelope ISRS response at 5% damping at the roof of the instrumented building with the empirical ISRS obtained from the procedure in IAEA TECDOC 348 (1985) and ASCE 7 (2022). The same figure also shows the envelope of the building input spectra at the foundation elevation. Given the low magnitude of the earthquakes in Table 4, a damping ratio of 4% is assigned to the building in this case study.

Table 4: Earthquakes with Available Acceleration Data in CESMD (2022) for the Instrumented Building

Earthquake Name	Date	Magnitude	Ground PGA (g)
Maricopa	08 May 2010	4.3ML	0.010
Isla Vista	29 May 2013	4.8ML	0.006
Wasco	24 February 2016	4.9MW	0.012
Ridgecrest	6 July 2019	7.1MW	0.009
Lone Pine	24 June 2020	5.8MW	0.005

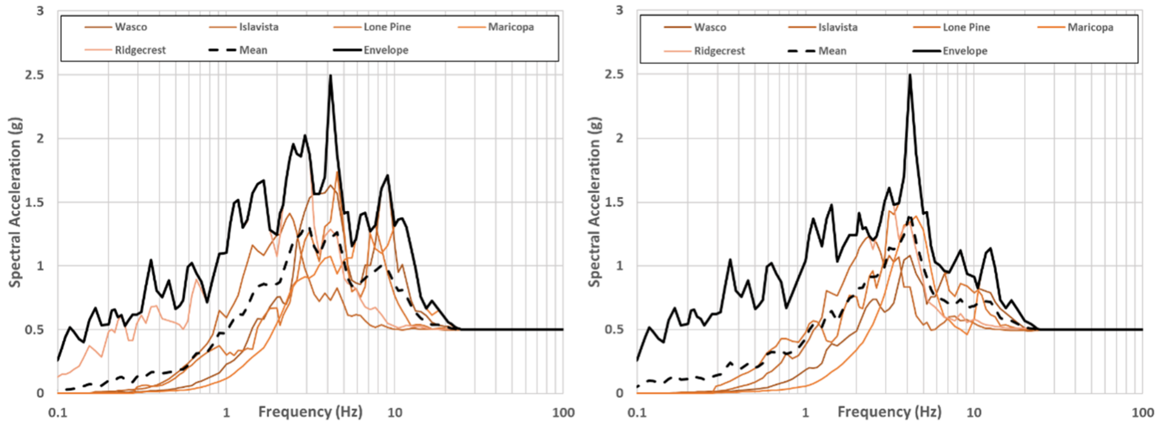

Figure 6. 5% Damping Scaled Response Spectra from Various Earthquakes at the Foundation of the Instrumented Building, N-S Direction (Left) and E-W Direction (Right)

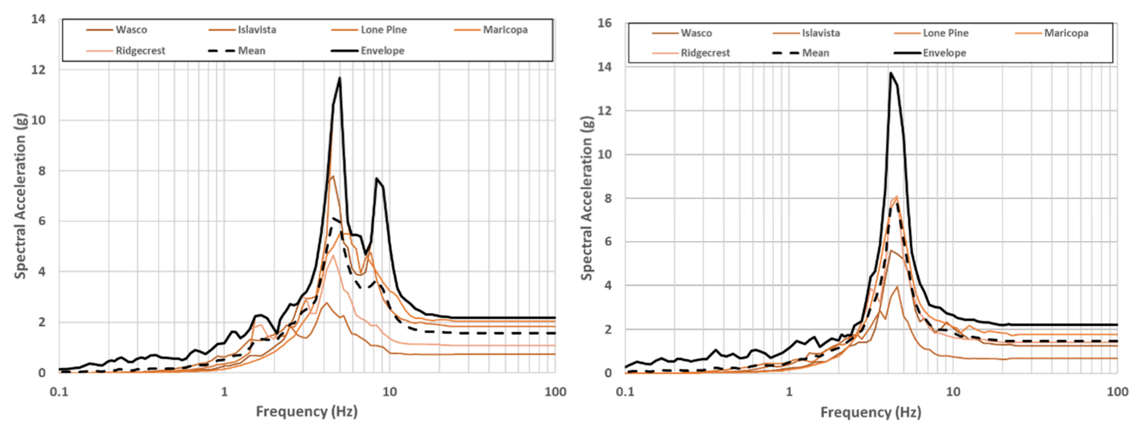

Figure 7. 5% Damping Scaled ISRS from Various Earthquakes at the Roof of the Instrumented Building, N-S Direction (Left) and E-W Direction (Right)

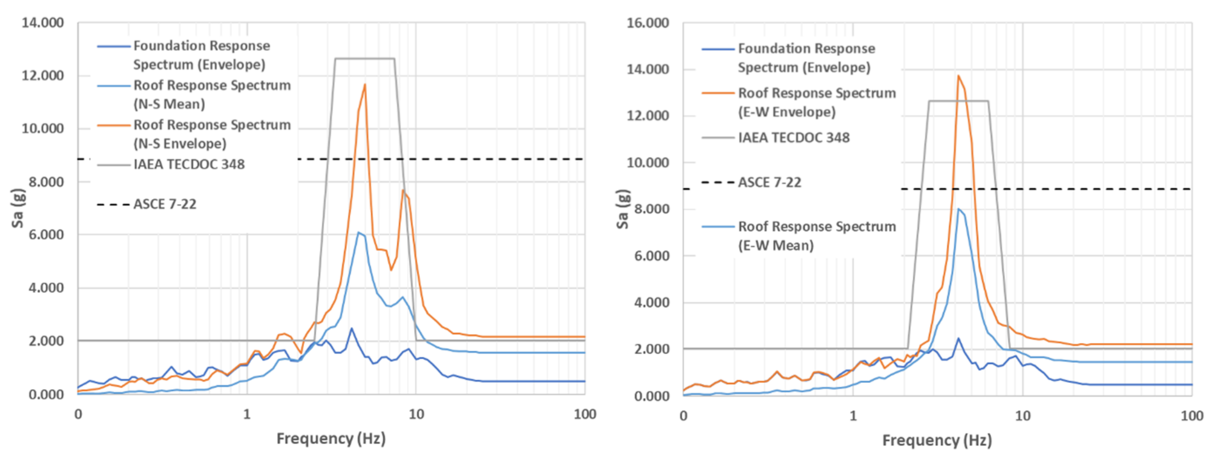

Figure 8. Comparison of the 5% Damping Scaled ISRS Obtained from the Recorded Accelerations with the Empirical Methods and the Foundation Input Spectra, N-S Direction (Left) and E-W Direction (Right)

As can be observed, the IAEA-TECDOC-348 (1985) method results in similar peak spectral accelerations to the envelope of the scaled ISRS. Considering that the shape of the ISRS from the five acceleration records are reasonably similar, the envelope of the scaled ISRS can be considered as the design (or 80th percentile) ISRS. The PGA of the ISRS from IAEA-TECDOC-348 PGA is also fairly close to the envelope of the PGA obtained from recorded earthquakes. On the other hand, the ASCE 7 (2022) method significantly underestimates the peak spectral acceleration for this building. As can be seen, the peak spectral acceleration from ASCE 7 (2022) is between 25% to 35% below the recorded envelope of the measured peak spectral acceleration in this case. Is it possible that this underestimation is because ASCE 7 (2022) is considering overstrength and ductility in response, whereas the empirical earthquakes are low enough amplitude that the structure is responding essentially elastically. Additionally, the ASCE 7's equation is intended to predict the inertia force applicable for the design of equipment, which may be different from the peak of the ISRS (i.e., the response of the instrumented building). For example, Section 6.2.3 of ASCE 4 (2016) allows for a 15% peak reduction for narrow frequency peak amplitudes for analysis of sub-systems. Considering a 15% reduction in the peak of the measured response spectra would provide a favorable comparison with the peak spectral acceleration of ASCE 7 (2022).

CONCLUSIONS

This paper compares the ISRS obtained from probabilistic transient analyses of the numerical model of an example nuclear plant low-rise shear-wall structure and the ISRS obtained from the recorded accelerations in an instrumented low-rise shear-wall building with those from standards-based simplified empirical methods outlined in IAEA-TECDOC-348 (1985) and ASCE 7 (2022). Since the empirical methods and the instrumentation data were primarily available for the horizontal response at the time of writing this paper, this study considers horizontal response only, and the evaluation of the vertical response is not part of the current study.

The results indicate that the IAEA-TECDOC-348 (1985) empirical method can predict the ISRS response of both the numerical model and the instrumented building well and may therefore have broader opportunities for use in lieu of time-consuming detailed SSI analyses.

While the peak spectral acceleration obtained from the ASCE 7 (2022) procedure is reasonably comparable to the results of the numerical model, it underestimates the narrow-band measured response of the instrumented building by about 25% to 35%. Is it possible that this underestimation is because ASCE 7 (2022) is considering overstrength and ductility in the response estimate, whereas the empirical earthquakes are low enough amplitude that the structure is responding essentially elastically. Moreover, given the narrow-band frequency of the measured roof response spectra, a 15% peak reduction for narrow frequency peak amplitudes is permissible in ASCE 4 (2016), and would provide a more favorable comparison with the peak spectral acceleration of ASCE 7 (2022).

These conclusions may be case-specific, such that generalized conclusions are not appropriate from the limited exploration and case studies presented here. Additional sensitivity studies and more in-depth evaluation are recommended. However, preliminary insights suggest that it may be feasible to utilize a more simplified consideration of in-structure seismic demands on nuclear facility equipment than detailed dynamic transient and still achieve equivalent seismic safety.

REFERENCES

American Society of Civil Engineers, (2016). "ASCE/SEI 4-16 standard for Seismic Analysis of Safety-Related Nuclear Structures," American Society of Civil Engineers, Reston, VA, USA.

American Society of Civil Engineers, (2022). "ASCE/SEI 7-22 Standard for Minimum Design Loads and Associated Criteria for Buildings and Other Structures," American Society of Civil Engineers, Reston, VA, USA.

American Society of Civil Engineers, (2022). ASCE Hazard Tool webpage https://asce7hazardtool.online. Accessed on March 2022.

Center for Engineering Strong Motion Data, (2022.) Strong-motion data set webpage: www.strongmotioncenter.org. Accessed on March 2022.

International Atomic Energy Agency, (1985). "Report No. IAEA-TECDOC-348. Earthquake Resistant Design of Nuclear Facilities with Limited Radioactive Inventory," International Atomic Energy Agency, Vienna, Austria.

National Institute of Standards and Technology, GCR 18-917-43, (2018). "Recommendations for improved seismic design and installation of non-structural components," Applied Technology Council, Redwood, CA.